Ocean Modelling 174 (2022) 102013

Contents lists available at ScienceDirect

Ocean Modelling

journal homepage: www.elsevier.com/locate/ocemod

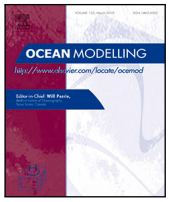

On the coupling between surface waves and the motion in a flexible porous surface layer

Jan Erik H. Weber

Department of Geosciences, University of Oslo, Oslo, Norway

ARTICLE INFO

Keywords:
Damped surface gravity waves
Porous floating surface layer
Rubble ice
Wave-induced Lagrangian mean drift

ABSTRACT

The coupling between surface waves and the motion in a flexible porous surface layer is investigated theoretically. We apply a Lagrangian formulation for the viscous fluid and the fluid-saturated porous medium. In the floating porous layer, which we assume to be much thinner than the wavelength, we apply a macroscopic version of Darcy's law. The interface between the porous layer and the underlying fluid is permeable, and the wave-induced vertical motion at the interface leads to wave damping. In addition, the viscous shear stress at the interface also dampens the waves. We here investigate the relative strength of the two mechanisms. Furthermore, we calculate the Lagrangian mean drift in the porous surface layer. The present study may provide a physical model for wave damping in the presence of unconsolidated rubble ice and the slow particle drift in rubble-ice layers.

1. Introduction

In a pioneering paper (Reid and Kajiura, 1957) the linear interaction between surface wave motion in a fluid layer of finite depth, and the motion in an underlying saturated porous medium of infinite depth, is investigated. The fluid is inviscid and the flow in the porous medium is governed by Darcy's law. It is found that the vertical flow at the boundary between the porous bed and the overlying fluid causes the waves to become spatially attenuated. Later works (Webber and Huppert, 2020, 2021; Weber and Ghaffari, 2021) have studied the associated nonlinear mean drift in a porous seabed of finite thickness when the ocean wave motion is irrotational.

The present investigation takes this problem further by considering the coupling between deep-water gravity waves and a thin floating flexible porous layer. Again, as in the bottom layer case, there will be a wave-induced vertical motion at the boundary between the porous layer and the fluid, leading to wave damping. Here we assume that the ocean is viscous, and the viscous shear stress at the interface (Beavers and Joseph, 1967; Jones, 1973) leads to an additional damping of the wave motion. In this paper, we investigate the relative strength of the two mechanisms. Furthermore, we calculate the Lagrangian mean drift in the porous surface layer.

Since the thickness of the viscous boundary layer in the fluid is very much smaller than the wave amplitude, one should apply a curvilinear type of coordinate system to describe the motion for small, but finite wave amplitudes. In the present paper, this is achieved by describing the fluid motion in Lagrangian particle-following coordinates. Since the pressure gradient becomes nonlinear in this description, the procedure has the additional advantage that the wave-drift terms now appears directly in the Darcy equation for the porous flexible layer.

The rest of this article is organized as follows: In Section 2, we describe the mathematical formulation, and in Section 3, we present results from a linear analysis. In Section 4, we discuss the possible application of our theory to rubble ice. In Section 5, we derive the Lagrangian mean drift in the porous layer, while Section 6 contains a discussion and some concluding remarks.

2. Mathematical formulation

We study surface gravity waves in an ocean of unlimited depth. The effect of the Earth's rotation is neglected, and the motion is two-dimensional. At the surface, we have a floating fluid-saturated thin flexible porous layer of initial thickness H_1. We take that the X-axis is horizontal and situated at the undisturbed interface between the porous layer and the infinitely deep fluid, while the Z-axis is vertical and directed upwards. The fluid is incompressible with constant density ρ in the porous medium and in the fluid below. Upper and lower layer variables are denoted by subscripts 1 and 2, respectively. The material upper surface is found at $Z_1 = H_1 + \eta_1$, and the position of the water surface (the interface) is $Z_2 = \eta_2$; see Fig. 1. The lower boundary is situated very far from the surface. Here, mathematically, $Z_2 \to -\infty$.

The infinitely deep ocean is taken to be a Newtonian viscous fluid, which makes the wave motion rotational. In the porous medium, the motion is dominated by friction. We here consider a porous medium where the pore dimension is not necessarily microscopic. Such larger scales may, for example, be found in floating vegetation mats with a

E-mail address: j.e.weber@geo.uio.no.

https://doi.org/10.1016/j.ocemod.2022.102013
Received 10 March 2022; Received in revised form 4 April 2022; Accepted 28 April 2022
Available online 4 May 2022

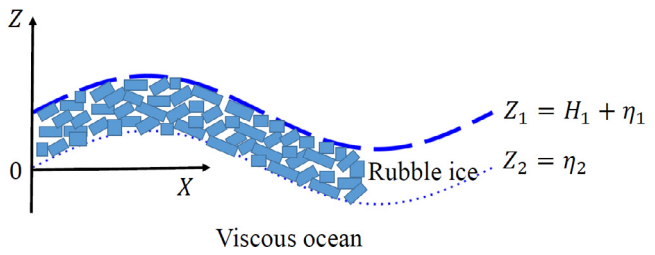

Fig. 1. A diagram showing the configuration, with a surface wave beneath a flexible water-saturated porous layer. The layer thickness in the absence of waves is H_1. In the figure, the porous medium is depicted schematically as a rubble-ice layer with reference to the application in Section 4 and further on.

fibrous structure, or in rubble ice as indicated in Fig. 1. In the present study, we apply a rather simple model for the flow in the porous medium, assuming that the Reynolds-averaged Navier–Stokes (RANS) equations are valid in the voids. By averaging the RANS equations over a representative elementary volume of the porous medium domain, a macroscale equation for the momentum balance is obtained, with an effective permeability K and an eddy viscosity ν_1; see e.g. Masuoka and Takatsu (1996). To the lowest order approximation, Darcy's law (Bear, 1972) then applies to the motion in the macroscopic porous medium.

As explained in the Introduction, we apply Lagrangian coordinates for the mathematical analysis. Let a fluid particle (a, c) initially have coordinates (X_0, Z_0). Its position (X, Z) at later times will then be a function of a, c and time t. Velocity components and accelerations are given by (X_t, Z_t) and (X_{tt}, Z_{tt}), respectively, where subscripts denote partial differentiation and the pressure is P. The transformation of X, Z from independent variables in the Eulerian description to dependent Lagrangian variables $X(a, c, t)$, $Z(a, c, t)$ is trivial; see Lamb (1932).

We consider a thin flexible porous layer, and assume that the balance of forces in the vertical direction is hydrostatic. Furthermore, we take that the pressure is constant along the upper surface. Then we have for the pressure distribution in the porous layer

$$P_1/\rho = -g(Z_1 - H_1 - \eta_1), \tag{1}$$

where g is the acceleration due to gravity, and an insignificant constant has been put equal to zero.

In Lagrangian coordinates, Darcy's law can be written (Weber and Ghaffari, 2021),

$$(\nu_1/K)X_{1t}X_{1a} = -g\eta_{1a}. \tag{2}$$

Here K is the permeability in the horizontal direction, and ν_1 is the kinematic viscosity of the fluid in the voids. We note from (2) that X_1 is only a function of a and t.

The momentum balance in the fluid can be written in Lagrangian notation from Lamb (1932), by adding the viscous terms:

$$X_{2tt}X_{2a} + Z_{2tt}Z_{2a} + gZ_{2a} = -P_{2a}/\rho + \nu_2[X_{2a}\nabla^2 X_{2t} + Z_{2a}\nabla^2 Z_{2t}], \tag{3}$$

$$X_{2tt}X_{2c} + Z_{2tt}Z_{2c} + gZ_{2c} = -P_{2c}/\rho + \nu_2[X_{2c}\nabla^2 X_{2t} + Z_{2c}\nabla^2 Z_{2t}], \tag{4}$$

where ν_2 is the constant eddy viscosity in the fluid. The Laplacian operator ∇^2 is non-linear in the Lagrangian formulation; see for example Pierson (1962) for the explicit form.

Finally, since the density is constant and the same in each layer, the conservation of mass (now volume) can be written in both layers as

$$J(X, Z) = J(X_0, Z_0). \tag{5}$$

Here $J(F, G) \equiv F_a G_c - F_c G_a$ is the two-dimensional Jacobian.

Even though (a, c) is not the initial particle position, it is convenient to write the displacements and pressure as (Pierson, 1962):

$$\left.\begin{aligned} X_1 &= a + x_1(a, t), \\ Z_1 &= c + z_1(a, c, t), \\ P_1 &= -\rho g(c - H_1) + p_1(a, c, t). \end{aligned}\right\} \quad 0 \le c \le H_1, \tag{6}$$

$$\left.\begin{aligned} X_2 &= a + x_2(a, c, t), \\ Z_2 &= c + z_2(a, c, t), \\ P_2 &= -\rho g(c - H_1) + p_2(a, c, t). \end{aligned}\right\} \quad c \le 0. \tag{7}$$

The deviations $(x_{1,2}, z_{1,2}, p_{1,2})$ in (6)–(7) can be expanded in series after a small parameter ϵ proportional to the wave amplitude; see e.g. Weber (2019). Accordingly, (2)–(5) can be written

$$(\nu_1/K)x_{1t}(1 + x_{1a}) = -\left(p_1/\rho + gz_1\right)_a = -g\eta_{1a}, \tag{8}$$

$$x_{2tt}(1 + x_{2a}) + z_{2tt}z_{2a} = -\left(p_2/\rho + gz_2\right)_a + \nu_2[(1 + x_{2a})\nabla^2 x_{2t} + z_{2a}\nabla^2 z_{2t}], \tag{9}$$

$$x_{2tt}x_{2c} + z_{2tt}(1 + z_{2c}) = -\left(p_2/\rho + gz_2\right)_c + \nu_2[x_{2c}\nabla^2 x_{2t} + (1 + z_{2c})\nabla^2 z_{2t}], \tag{10}$$

$$x_{1,2ta} + z_{1,2tc} + (x_{1,2a}z_{1,2c})_t - (x_{1,2c}z_{1,2a})_t = 0. \tag{11}$$

With this notation we have that $\eta_1(a, t) = z_1(a, H_1, t)$ and $\eta_2(a, t) = z_2(a, 0, t)$ in Fig. 1.

3. Linear analysis

3.1. Porous layer

We linearize our governing equations (8)–(11), and denote our linearized variables by a tilde. In the porous layer we have

$$(\nu_1/K)\tilde{x}_{1t} = -g\tilde{\eta}_{1a}. \tag{12}$$

We take that

$$\tilde{\eta}_1 = \eta_0 \exp i(\kappa a - nt), \tag{13}$$

where η_0 is the real wave amplitude, and

$$\kappa = k + i\alpha, \tag{14}$$

$$n = \omega - i\beta. \tag{15}$$

Here k is the real wave number, and ω the wave frequency, while α and β are the spatial and temporal damping coefficients, respectively. We assume slow damping, i.e. $\alpha/k \ll 1$ and $\beta/\omega \ll 1$. From (12),

$$\tilde{x}_1 = g\kappa K\tilde{\eta}_1/(n\nu_1). \tag{16}$$

Then, from (11),

$$\tilde{z}_{1tc} = -\tilde{x}_{1ta} = -g\kappa^2 K\tilde{\eta}_1/\nu_1. \tag{17}$$

At the upper boundary, we have $\tilde{z}_1(c = H_1) = \tilde{\eta}_1$. Accordingly:

$$\tilde{z}_1 = \left[1 + ig\kappa^2 K\left(H_1 - c\right)/\left(n\nu_1\right)\right]\tilde{\eta}_1. \tag{18}$$

3.2. Viscous fluid

In the fluid the linearized equations become

$$\tilde{x}_{2tt} = -\left(\tilde{p}_2/\rho + g\tilde{z}_2\right)_a + \nu_2\nabla_L^2\tilde{x}_{2t} \tag{19}$$

$$\tilde{z}_{2tt} = -\left(\tilde{p}_2/\rho + g\tilde{z}_2\right)_c + \nu_2\nabla_L^2\tilde{z}_{2t}, \tag{20}$$

where $\nabla_L^2 = \partial^2/\partial a^2 + \partial^2/\partial c^2$. From Lamb (1932), we introduce

$$\tilde{x}_{2t} = -\tilde{\varphi}_a - \tilde{\psi}_c, \tag{21}$$

$$\tilde{z}_{2t} = -\tilde{\varphi}_c + \tilde{\psi}_a. \tag{22}$$

Then (19)–(20) and the linearized version of (11), yield that

$$\nabla_L^2\tilde{\varphi} = 0, \tag{23}$$

$$\tilde{\psi}_t - \nu_2\nabla_L^2\tilde{\psi} = 0, \tag{24}$$

$$\tilde{p}_2/\rho = \tilde{\varphi}_t - g\tilde{z}_2. \tag{25}$$

Assuming that $\tilde{\varphi}, \tilde{\psi} \to 0$, when $c \to -\infty$, we find

$$\tilde{\varphi} = A_2 \exp(\kappa c + i(\kappa a - nt)), \tag{26}$$

$$\tilde{\psi} = B_2 \exp(mc + i(\kappa a - nt)), \tag{27}$$

where

$$m = (1-i)\gamma. \tag{28}$$

Here the large parameter γ is given by $\gamma = \left[\omega/(2\nu_2)\right]^{1/2}$.

3.3. Boundary conditions

With an upper porous layer, we have a discontinuity in the horizontal velocities at the interface. The vertical velocity, however, must be continuous; see for example the discussion in Webber and Huppert (2021). Hence,

$$\tilde{z}_1(c=0) = \tilde{z}_2(c=0). \tag{29}$$

Furthermore, with a viscous fluid beneath the porous layer, the horizontal stress in the fluid cannot vanish at the interface. From Beavers and Joseph (1967) and Jones (1973), we have that

$$\tilde{x}_{2tc} + \tilde{z}_{2ta} = (a_{BJ}/K^{1/2})(\tilde{x}_{2t} - \tilde{x}_{1t}), \qquad c = 0. \tag{30}$$

Here a_{BJ} is the dimensionless Beavers–Joseph parameter, which depends on the pore-space geometry of the porous medium. Experimental studies by Beavers and Joseph (1967) indicate that this parameter is in the range $0.1-4.0$, where the largest values of a_{BJ} occur for the largest pore diameter.

Finally, the normal stresses must be continuous at the interface, i.e.

$$-\tilde{p}_1 = -\tilde{p}_2 + 2\rho\nu_2\tilde{z}_{2tc}, \quad c = 0. \tag{31}$$

Here $\tilde{p}_1 = -\rho g(\tilde{z}_1 - \tilde{\eta}_1)$ from (1), while $\tilde{p}_2$ is given by (25). Utilizing (29), we find from (31) that

$$\tilde{\varphi}_t - 2\nu_2\tilde{z}_{2tc} - g\tilde{\eta}_1 = 0, \quad c = 0. \tag{32}$$

From the kinematic condition (29) we obtain

$$A_2 - iB_2 = (in/\kappa)[1 + i\kappa^2 g H_1 K/(n\nu_1)]\eta_0, \tag{33}$$

while (30) yields that

$$\omega\kappa(q_1 - 2\kappa)A_2 + i\omega m(m - q_1)B_2 = g\kappa q_2\eta_0. \tag{34}$$

Here we have defined the material constants q_1 and q_2 by

$$q_1 = a_{BJ}/K^{1/2}, \tag{35}$$

$$q_2 = a_{BJ}\omega K^{1/2}/\nu_1, \tag{36}$$

while m is defined by (28).

Finally, from (32) we find that

$$\left(-in + 2\kappa^2\nu_2\right)A_2 - 2i\kappa m\nu_2 B_2 = g\eta_0. \tag{37}$$

In solving the system of Eqs. (33), (34) and (37), where η_0 is given, we utilize the fact that

$$k/\gamma \ll 1, \tag{38}$$

$$k/q_1 \ll 1. \tag{39}$$

Furthermore,

$$R = \omega K/\nu_1 = q_2/q_1 \ll 1. \tag{40}$$

Here (38) follows from the fact that the viscous boundary layer is very thin and (39) from the fact that the permeability of the porous medium is small. Finally, R in (40) is a small fundamental parameter in the porous problem, as first pointed out by Reid and Kajiura (1957).

It is readily shown that to lowest order, (33) and (34) yield the obvious result $\omega^2 = gk$. Utilizing this fact, we obtain to next order,

$$A_2 = (i\omega - \beta)(\eta_0/k), \tag{41}$$

$$B_2 = i(2\beta + \omega\alpha/k - \omega k H_1 R)(\eta_0/k). \tag{42}$$

Finally, by inserting these results into (34), we find from the real part that

$$\beta + c_g\alpha = \omega k[q_1^2 + 2\gamma q_2 - q_1 q_2]/[4\gamma\left(q_1^2 + 2\gamma^2 - 2\gamma q_1\right)] + \omega k H_1 R/2 = Q, \tag{43}$$

where $c_g = \omega/(2k)$ is the group velocity for deep-water gravity waves. Here (43) is just a special version of the general form relating temporal and spatial wave damping to the dissipative process in the wave motion Weber (2022). Specifically, we note from (43) that if $\alpha = 0$ (temporal attenuation), then $\beta = Q$. If $\beta = 0$ (spatial attenuation), then $\alpha = Q/c_g$. Accordingly, when comparing the two different cases, we have $\beta = c_g\alpha$, as shown by Gaster (1962).

We can non-dimensionalize (43) by scaling the temporal wave damping by the inextensible film limit $\beta_{inex} = \omega k/(4\gamma)$ (Lamb, 1932). This is the case where the water particles in contact with the surface cover have zero horizontal velocity. Introducing $\hat{\beta} = \beta/\beta_{inex}$ and $\hat{\alpha} = 4\gamma\alpha/k^2$, (43) becomes

$$\hat{\beta} + \frac{1}{2}\hat{\alpha} = (q_1^2 + 2\gamma q_2 - q_1 q_2)/\left(q_1^2 + 2\gamma^2 - 2\gamma q_1\right) + 2\gamma H_1 R = Q_1 + Q_2. \tag{44}$$

Here Q_1 represents the wave damping caused by friction, while Q_2 models the damping caused by vertical motion at the interface between the porous layer and the fluid. We shall refer to the two mechanisms as viscous and porous damping, respectively. As mentioned in the Introduction, the latter damping mechanism was first described for an infinitely deep porous seabed by Reid and Kajiura (1957).

4. Application to rubble ice

Rubble ice is produced when ice floes collide, leading to smaller pieces of broken ice. Such formation also occurs when ice collides with offshore structures, or when ships pass through an ice cover; see the comprehensive review of field observations by Strub-Klein and Sudom (2012). The rubble layer consists of randomly orientated elongated ice blocks with water in the voids between them; see the sketch in Fig. 1. On top, there is usually a thinner layer of consolidated ice. As the freezing season progresses, the rubble layer may partly refreeze.

The dimensions of the rubble blocks are related to the thickness of the ice floes that break up, i.e. thicker ice, larger rubble. As inferred from Strub-Klein and Sudom (2012), a typical block thickness d could be of the order 0.5 m with lateral dimensions $2d - 3d$. The thickness of the rubble layer is several times the thickness of the consolidated ice on top. From field measurements in the Barents Sea, the permeability of rubble ice appears to be of order $10^{-8}\,\mathrm{m}^2$ (Marchenko, 2022), while Freitag and Eicken (2003) report values up to $10^{-7}\,\mathrm{m}^2$ (it should be mentioned that these values refer to permeability in the vertical direction).

In calculating the right-hand side of (44), we assume that we have a moderately large eddy viscosity in the ocean beneath the ice; see Weber (1987), or Melsom (1992). Also in the rubble, we take that the viscosity is somewhat larger than the molecular value. Furthermore, we assume from Beavers and Joseph (1967) that $a_{BJ} = 4.0$ in (35)–(36). This choice is not very sensitive, and a ten times higher value does not change the results. Accordingly, for the calculation of the right-hand side of (44), we take that $\nu_1 = 5 \cdot 10^{-6}\,\mathrm{m}^2\mathrm{s}^{-1}$, $\nu_2 = 10^{-4}\,\mathrm{m}^2\mathrm{s}^{-1}$, $K = 5 \cdot 10^{-8}\,\mathrm{m}^2$, $H_1 = 2\,\mathrm{m}$ and $a_{BJ} = 4.0$. It is seen that with these values, the conditions (38)–(40) are very well fulfilled. In Fig. 2, we have displayed Q_1 and Q_2 from (44) as function of the wavelength $\lambda = 2\pi/k$.

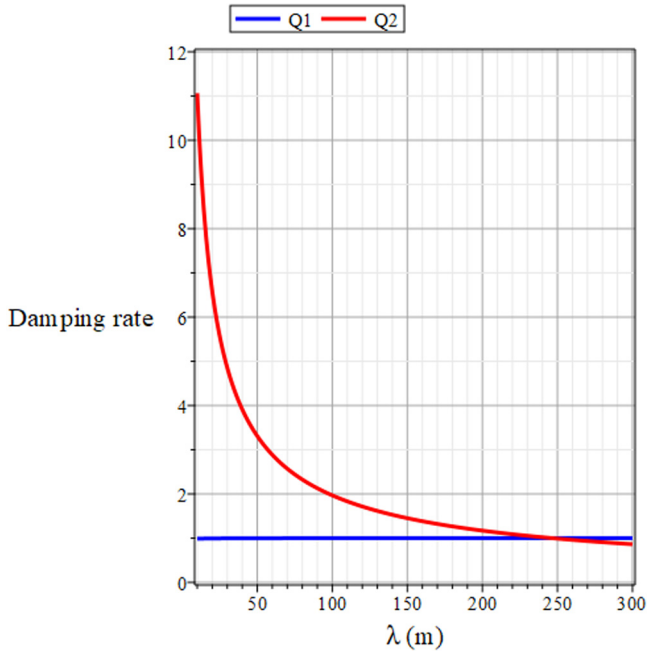

Fig. 2. Non-dimensional damping rates Q_1 (blue line) and Q_2 (red line) as function of the wavelength.

We note from the figure that porous damping (red line) is considerably larger than viscous damping (blue line) for shorter waves in this example. From (30) we see that for large values of q_1, we have that $\tilde{x}_{2t} \to 0$ when $c = 0$. This corresponds to the inextensible layer limit (Lamb, 1932). This is actually the case for the whole wave number range in Fig. 2, making $Q_1 \approx 1$, as seen from (44). We realize from Fig. 2 that the porous damping mechanism very effectively filters out smaller waves from the wave spectrum as the surface wave propagate from the open sea into the ice pack. We have here assume that the thin layer of consolidated is broken up on the wave scale. Hence, we can neglect the elastic properties of the consolidated ice (Liu and Mollo-Christensen, 1988; Melsom, 1992).

It should be stressed that the porous damping effect is related to the small parameter $R = \omega K/\nu_1$. Hence, a smaller value of ν_1 (a molecular value), or a larger permeability will enhance the numerical values of the damping rates considerably.

5. The Lagrangian mean drift

Here we consider the nonlinear problem to second order for the Lagrangian mean quantities. The mean is defined by averaging over the wave cycle, and this process is denoted by an over-bar. We find to second order, when averaging (8) in the porous layer,

$$u_1^{(L)} = -\overline{\tilde{x}_{1t}\tilde{x}_{1a}} - (gK/\nu_1)\overline{\eta}_{1a}, \tag{45}$$

where $u_1^{(L)} = \overline{x}_{1t}$ is the horizontal Lagrangian mean drift in the porous medium. The Stokes drift (Stokes, 1847) to second order in Eulerian variables was derived by Longuet-Higgins (1953). In Lagrangian terms, Longuet-Higgins' formula can be written

$$u_1^{(S)} = \overline{\tilde{x}_1\tilde{x}_{1ta}} + \overline{\tilde{z}_1\tilde{x}_{1tc}}. \tag{46}$$

Since $\tilde{x}_1 = \tilde{x}_1(a,t)$; see (6), we find from (46) that in the porous layer

$$u_1^{(S)} = \left(\overline{\tilde{x}_{1t}\tilde{x}_1}\right)_a - \overline{\tilde{x}_1\tilde{x}_{1ta}} = -\overline{\tilde{x}_1\tilde{x}_{1ta}}, \tag{47}$$

since $\left(\overline{\tilde{x}_{1t}\tilde{x}_1}\right)_a$ is very small (of $O(\alpha\beta)$). Hence, we can write (45) as

$$u_1^{(L)} = u_1^{(S)} + u_1^{(E)}, \tag{48}$$

where

$$u_1^{(E)} = -(gK/\nu_1)\overline{\eta}_{1a} \tag{49}$$

is the Eulerian mean velocity. We see right away that for purely temporal decay ($\alpha = 0$), we have that $u_1^{(E)} = 0$.

In calculating the wave damping (43), the ocean was assumed to be a viscous fluid. Fig. 2 shows that the viscous effect alone on damping was equivalent to assuming an inextensible layer at the surface. The associated Lagrangian mean current in the viscous ocean in this case has been thoroughly discussed in Weber (1987). The new element in this paper is porous damping, which operates independently of the oceanic eddy viscosity. It yields considerably larger wave damping than viscosity, as seen in Fig. 2. We therefore focus on this effect on the drift velocity and neglect viscosity in the ocean in this last part of our study. With this assumption, we obtain from (9) that

$$u_{2t}^{(L)} = -\overline{\tilde{x}_{2tt}\tilde{x}_{2a}} - \overline{\tilde{z}_{2tt}\tilde{z}_{2a}} - (\overline{p}_2/\rho + g\overline{z}_2)_a, \tag{50}$$

where $u_2^{(L)} = \overline{x}_{2t}$ is the horizontal Lagrangian mean drift. We require a steady Lagrangian mean drift. Then, the right-hand side of (50) must vanish. Accordingly,

$$(\overline{p}_2/\rho + g\overline{z}_2)_a = -\overline{\tilde{x}_{2tt}\tilde{x}_{2a}} - \overline{\tilde{z}_{2tt}\tilde{z}_{2a}} = -\alpha\omega^2(\overline{\tilde{x}_2^2} + \overline{\tilde{z}_2^2}), \tag{51}$$

where the last result is correct to lowest order. At the interface we must have continuity of pressure and the mean elevation, i.e. $\overline{p}_1(c=0) = \overline{p}_2(c=0)$ and $\overline{z}_1(c=0) = \overline{z}_2(c=0)$. Hence,

$$(\overline{p}_1/\rho + g\overline{z}_1)_a = (\overline{p}_2/\rho + g\overline{z}_2)_a, c = 0. \tag{52}$$

Inserting from (8) and (51), we find that

$$g\overline{\eta}_{1a} = -\alpha\omega^2(\overline{\tilde{x}_2^2} + \overline{\tilde{z}_2^2}), c = 0. \tag{53}$$

When we neglect the effect of viscosity in the fluid, we have from (21)–(22) that $\tilde{x}_{2t} = -\tilde{\varphi}_a$, and $\tilde{z}_{2t} = -\tilde{\varphi}_c$, where $\tilde{\varphi}$ is given by (26). Here, to lowest order from (41), $A_2 = i\omega\eta_0/k$. Inserting real values into (53), we find that

$$g\overline{\eta}_{1a} = -\alpha\omega^2\eta_0^2\exp[-2(\alpha a + \beta t)]. \tag{54}$$

In this case, we obtain from (43) for the damping rates,

$$\beta + c_g\alpha = \omega k H_1 R/2, \tag{55}$$

where the small parameter R is given by (40). From (49) the Eulerian mean current becomes

$$u_1^{(E)} = \alpha\omega R\eta_0^2\exp[-2(\alpha a + \beta t)]. \tag{56}$$

Likewise, we find from (47) for the Stokes drift

$$u_1^{(S)} = \frac{1}{2}\omega k R^2\eta_0^2\exp[-2(\alpha a + \beta t)]. \tag{57}$$

Hence, the Lagrangian mean drift (48) becomes

$$u_1^{(L)} = \left[R/2 + \alpha/k\right]\omega k R\eta_0^2\exp[-2(\alpha a + \beta t)], \tag{58}$$

where the second term in the parenthesis is the Eulerian contribution. For spatially damped waves ($\beta = 0$), which is the relevant case for waves propagating inwards from the ice edge, we have from (55) that $\alpha = k^2 H_1 R$. Hence, (58) becomes

$$u_1^{(L)} = \left[1/2 + kH_1\right]\omega k R^2\eta_0^2\exp(-2\alpha a). \tag{59}$$

Since we have assumed that the porous layer is thin ($kH_1 \ll 1$), we note from the second term in (59) that the Eulerian contribution to the Lagrangian mean drift is small. Hence, pure temporal wave decay and pure spatial wave decay yield in practice the same mean drift current in the porous layer, being the Stokes drift.

In the fluid, we have assumed a non-accelerating mean drift, i.e. $u_{2t}^{(L)} = 0$ in (50). To derive an explicit expression for the steady Lagrangian mean velocity, we use the fact that the vorticity is zero in the fluid

in this non-viscous part of the study. Expressing the vorticity in Lagrangian terms, and assuming that the vorticity vanishes identically, we obtain from Weber (2011), Eq. (21) that

$$u_{2c}^{(L)} = 2\left(\overline{\tilde{x}\tilde{x}_{ta}} + \overline{\tilde{z}\tilde{x}_{tc}}\right) = 2ku_2^{(S)}. \tag{60}$$

Hence, in the infinitely deep fluid,

$$u_2^{(L)} = u_2^{(S)} = \omega k\eta_0^2 \exp[2kc - 2(\alpha a + \beta t)] \tag{61}$$

We remark that this result is also obtained if we use the Stokes drift expression (46) for the ocean. The difference here is that (61) yields the Lagrangian mean drift, so this equation tells us in addition that the Eulerian mean velocity vanishes in the inviscid ocean, which should not come as a surprise; see Longuet-Higgins (1953).

Spatial attenuation ($\alpha > 0$) introduces a small vertical mean drift into the problem. We obtain from the continuity Eq. (11) that $\overline{z}_{1tc} = -2\alpha\overline{x}_{1t}$, and $\overline{z}_{2tc} = -2\alpha\overline{x}_{2t}$. Assuming vanishing mean vertical velocity when $c \to -\infty$, we find for the fluid that

$$\overline{z}_{2t} = (\alpha/k)u_2^{(S)}, c \le 0. \tag{62}$$

Utilizing the continuity of mean velocities at $c = 0$, and neglecting a very small vertical creep of $O(R^3)$ within the medium, the interface and the porous layer will move upwards with a small velocity given by

$$\overline{z}_{1t} = (\alpha/k)u_2^{(S)}(c = 0). \tag{63}$$

We find that

$$\left|\overline{z}_{2t}/\tilde{z}_{2t}\right| = \alpha\eta_0 = (kH_1)R(k\eta_0), \tag{64}$$

where all of the three parts are much less than one. Hence, the vertical mean drift has no practical consequences in this problem.

6. Discussion and final remarks

We study the coupling between surface gravity waves and the motion in a floating flexible porous surface cover. As first shown by Reid and Kajiura (1957) for inviscid wave motion over a porous seabed, wave damping occurs due to the vertical flow at the boundary between the fluid and the porous bottom layer. As we have shown here, this phenomenon, which we have termed porous damping, also occurs when we have a floating porous layer at the sea surface.

Thin porous floating layers at the sea surface do occur in nature. The perhaps most fascinating example is the case of large mats of floating vegetation formed by *Sargassum* seaweed in the Sargasso Sea; see e.g. Gower and King (2011). These mats form a fibrous water-filled porous medium, which constitutes an important habitat for many marine species (it is sometimes referred to as the golden floating rainforest of the Atlantic Ocean). However, it is hard to find reports of physical properties such as porosity or permeability in the literature. Hence, without such data, our results will be rather speculative. On the other hand, with relevant data, the results reported in this paper could be applied to the slow flow of water (and pollution) in *Sargassum* seaweed cause by incoming surface waves.

We have therefore concentrated on the application to rubble-ice layers, which is a well-documented phenomenon in cold regions. This application is interesting in that porous damping acts stronger than viscous damping on shorter surface waves. It increases the filtering of shorter waves from wave spectra observed from platforms on the ice. However, also this case is not without problems. Since rubble ice often occurs beneath a layer of consolidated ice, the rubble is hard to observe from stations on the ice. Hence, it is difficult to separate the damping effect described here from other damping mechanisms in the vast amount of observations of waves in the ice; see for example Wadhams (2000), Squire (2020) and references therein.

In addition, the thickness of the rubble layer is not constant in real-world ice covers. It has maximum thickness beneath ice ridges; see for example Strub-Klein and Sudom (2012). On the other hand, Haapala (2000) reports of regions of fairly constant-thickness rubble ice in the Baltic Sea. Anyway, as long as the rubble layer is porous, some lateral variation in thickness will not obstruct the porous wave damping mechanism described here.

Finally, we remark that the porous matrix elements in ice rubble are not rigidly connected. However, we assume that the individual rubble blocks are so densely packed that we can ignore their relative motion. Furthermore, a precise description of the flow in the "pores" is probably not possible. But certainly, a kind of creeping motion will occur. Then, the Darcy formulation of the friction in the permeable medium may constitute a robust lowest order approximation; see also Marchenko (2022). The description of the slow Lagrangian mean transport in the rubble layer in this paper is new. It may have bearing to the motion of ice algae, or pollution like oil or microplastics in rubble ice.

Declaration of competing interest

The author declares that he has no known competing financial interests or personal relationships that could have appeared to influence the work reported in this paper.

Acknowledgments

Financial support from the Research Council of Norway through the Grant 280625 (Dynamics of floating ice) is gratefully acknowledged.

References

Bear, J., 1972. Dynamics of Fluids in Porous Media. American Elsevier Publ. Comp. NY..

Beavers, G.S., Joseph, D.D., 1967. Boundary conditions at a naturally permeable wall. J. Fluid Mech. 30, 197–207.

Freitag, J., Eicken, H., 2003. Meltwater circulation and permeability of Arctic summer sea ice derived from hydrological field experiments. J. Glaciol. 49, 349–358.

Gaster, M., 1962. A note on the relation between temporally-increasing and spatially-increasing disturbances in hydrodynamic stability. J. Fluid Mech. 14, 222–224.

Gower, J.F.R., King, S.A., 2011. Distribution of floating sargassum in the Gulf of Mexico and the Atlantic Ocean mapped using MERIS. Int. J. Rem. Sens. 32, 1917–1929.

Haapala, J., 2000. On the modelling of ice-thickness redistribution. J. Glaciol. 46, 427–437.

Jones, I.P., 1973. Low Reynolds number flow past a porous spherical shell. Proc. Camb. Phil. Soc. 73, 231–238.

Lamb, H., 1932. Hydrodynamics, 6th ed. Cambridge University Press, Cambridge, UK.

Liu, A.K., Mollo-Christensen, E., 1988. Wave propagation in a solid ice pack. J. Phys. Oceanogr. 18, 1702–1712.

Longuet-Higgins, M.S., 1953. Mass transport in water waves. Philos. Trans. Roy. Soc. Lond. A. 245, 535–581.

Marchenko, A., 2022. Thermo-hydrodynamics of sea ice rubble. In: Tuhkuri, J., Polojärvi, A. (Eds.), IUTAM Symposium on Physics and Mechanics of Sea Ice. In: IUTAM Bookseries, vol. 39, http://dx.doi.org/10.1007/978-3-030-80439-8_10.

Masuoka, T., Takatsu, Y., 1996. Turbulence model for flow through porous media. Int. J. Heat Mass Transfer 39, 2803–2809.

Melsom, A., 1992. Wave-induced roll motion beneath an ice cover. J. Phys. Oceanogr. 22, 19–28.

Pierson, W.J., 1962. Perturbation analysis of the Navier–Stokes equations in Lagrangian form with selected solutions. J. Geophys. Res. 67, 3151–3160.

Reid, R.O., Kajiura, K., 1957. On the damping of gravity waves over a permeable sea bed. Trans. Am. Geophys. Union. 38, 662–666.

Squire, V.A., 2020. Ocean wave interactions with sea ice: a reappraisal. Ann. Rev. Fluid Mech. 52, 37–60. http://dx.doi.org/10.1146/annurev-fluid-010719-060301.

Stokes, G.G., 1847. On the theory of oscillatory waves. Trans. Cam. Phil. Soc. 8, 441–455.

Strub-Klein, L., Sudom, D., 2012. A comprehensive analysis of the morphology of first-year sea ice ridges. Cold Reg. Sci. Technol. 82, 94–109.

Wadhams, P., 2000. Ice in the Ocean. Gordon and Breach Science Publ., ISBN: 90-5699-296-1, p. 351.

Webber, J.J., Huppert, H.E., 2020. Stokes drift in coral reefs with depth-varying permeability. Philos. Trans. R. Soc. A. 378, 20190531.

Webber, J.J., Huppert, H.E., 2021. Stokes drift through corals. Env. Fluid Mech. http://dx.doi.org/10.1007/s10652-021-09811-8.

Weber, J.E., 1987. Wave attenuation and wave drift in the marginal ice zone. J. Phys. Oceanogr. 17, 2351–2361.

Weber, J.E., 2011. Do we observe Gerstner waves in wave tank experiments? Wave Motion 48, 301–309.

Weber, J.E., 2019. Lagrangian studies of wave-induced flows in a viscous ocean. Deep-Sea Res. Part II. 160, 68–81.

Weber, J.E., 2022. A note on the temporal and spatial attenuation of ocean waves. Ocean Model. submitted to.

Weber, J.E., Ghaffari, P., 2021. Wave-induced Lagrangian drift in a porous seabed. Env. Fluid Mech. http://dx.doi.org/10.1007/s10652-021-09823-4.